Check for updates

View Article Online
View Journal

Journal of Materials Chemistry A

Accepted Manuscript

This article can be cited before page numbers have been issued, to do this please use: M. Tan, T. He, J. Liu, H. Wu, Q. Li, J. Zheng, Y. Wang, Z. Sun, S. Wang and Y. Zhang, *J. Mater. Chem. A*, 2018, DOI: 10.1039/C8TA01898G.

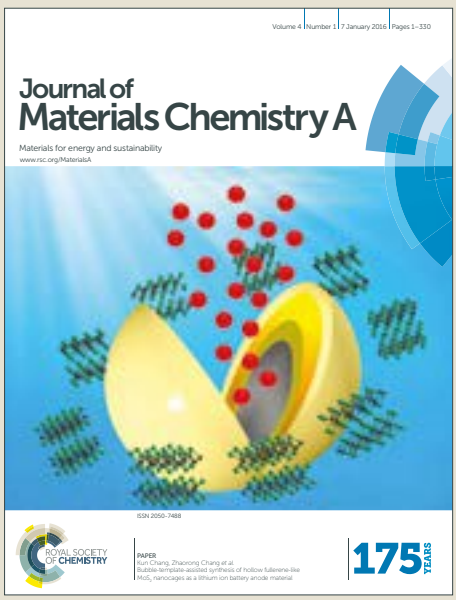

This is an Accepted Manuscript, which has been through the Royal Society of Chemistry peer review process and has been accepted for publication.

Accepted Manuscripts are published online shortly after acceptance, before technical editing, formatting and proof reading. Using this free service, authors can make their results available to the community, in citable form, before we publish the edited article. We will replace this Accepted Manuscript with the edited and formatted Advance Article as soon as it is available.

You can find more information about Accepted Manuscripts in the author guidelines.

Please note that technical editing may introduce minor changes to the text and/or graphics, which may alter content. The journal's standard Terms & Conditions and the ethical guidelines, outlined in our author and reviewer resource centre, still apply. In no event shall the Royal Society of Chemistry be held responsible for any errors or omissions in this Accepted Manuscript or any consequences arising from the use of any information it contains.

ROYAL SOCIETY OF CHEMISTRY

rsc.li/materials-a

View Article Online
DOI: 10.1039/C8TA01898G

Journal of Materials Chemistry A

COMMUNICATION

Supramolecular Bimetallogels: A Nanofiber Network for Bimetal/Nitrogen Co-Doped Carbon Electrocatalysts

Received 00th January 20xx,
Accepted 00th January 20xx

DOI: 10.1039/x0xx00000x

www.rsc.org/

Minli Tan,[a] Ting He,[a] Jian Liu,[a] Huiqiong Wu,[a] Qiang Li,[a] Jun Zheng,[a] Yong Wang,[a] Zhifang Sun,*[a] Shuangyin Wang[b] and Yi Zhang*[a]

This paper report a rational strategy, using 'supramolecular bimetallogel' as template, to synthesize a series of bimetal (Fe-Co, Fe-Ni or Fe-Mn)/nitrogen co-doped carbon electrocatalysts for ORR with excellent performance. The bimetallogel nanofiber network serves as both bimetal and N sources, as well as host matrix for the commercially available carbon. Thermal treatment of the bimetallogels enables a homogenous in-situ doping of the bimetal and N, affording bimetal/N co-doped carbon catalysts.

Rational design and synthesis of highly efficient and durable catalysts for oxygen reduction reactions (ORR) have exhibited considerable practical value for clean energy conversion systems, such as metal-air batteries and fuel cells.[1-4] Though precious metals, such as Pt-based materials, possess high electrocatalytic activity,[5-7] the prohibitive cost, scarcity and low stability greatly hinder their large-scale practical applications.[8-10] Recently, nonprecious metal-nitrogen-carbon nanocomposites (MNCs) show great potential as alternatives to Pt-based catalysts, but only rare examples exhibit superior activity and better durability than the Pt/C.[11-14] This dilemma comes with the methodology for the synthesis of MNCs, where high temperature annealing process is always required to pyrolyze a mixture of carbon sources, metal salts and nitrogen precursors.[15-17] During thermal treatment, these metal salts and nitrogen precursors easily agglomerate and resulted in inhomogeneous doping of metal and nitrogen into carbon matrix.[18-20] Traditionally, methodologies are overwhelmingly focusing on different combinations of mixtures containing carbon sources, metal ions and nitrogen-enriched molecules,[21-23] however, an important but often ignored aspect is that the structure and distribution of precursors, such as the geometric structures, can exert great effect on the composition and catalytic activity of the final products.[24-26] So far, despite of their great practical potential, it is still challenging to rational design and synthesis of highly active nonprecious metal-nitrogen-carbon nanocomposites for ORR.

In the previous work, we have reported that a supramolecular metallogelator, ferrocenoyl-phenylalanine (Fc-F), could undergo hierarchical self-assembly to form supramolecular hydrogel composed of well-defined three-dimensional nanofibers.[27] These nanofibers contain large amount of Fe and N as the metallogelator Fc-F was synthesized by condensation of ferrocene and amino acid moieties. In the present study, we found that the Fc-F, containing -COOH and -CO-NH- groups, could further coordinate with other transition metal ions (Co, Ni or Mn) and self-assembled into bimetallogels (their corresponding bimetallogels are denoted as Fc-F/Co, Fc-F/Ni and Fc-F/Mn, respectively). The bimetallogel nanofiber network could serve as bimetal and nitrogen sources, as well as host matrix to accommodate the commercially available carbon, Ketjenblack EC 600J, to form a hybrid hydrogel (denoted as Fc-F/Co@C, Fc-F/Ni@C and Fc-F/Mn@C, respectively). Using this hybrid bimetallogel as template, we were able to obtained a series of bimetal /nitrogen co-doped carbon electrocatalysts for ORR. To test this strategy, we chosen the Fc-F/Co@C gel as a model material for further investigation and elucidated the structure-

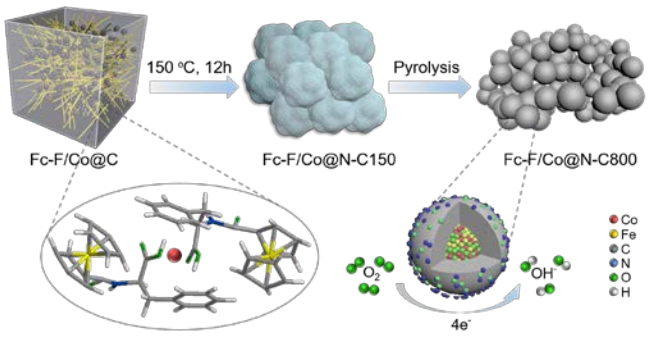

Scheme 1. Schematic representation for the synthesis of Fc-F/Co@N-C800 as efficient ORR catalysts.

[a] Hunan Provincial Key Laboratory of Efficient and Clean Untilization of Manganse Resources, College of Chemistry and Chemical Engineering, Central South University, Changsha 410083, China. E-mail: allensune@gmail.com (Z. Sun); yzhangcsu@csu.edu.cn (Y. Zhang)
[b] State Key Laboratory of Chem/Bio-Sensing and Chemometrics, Hunan University, Changsha 410082, China

† Footnotes relating to the title and/or authors should appear here.
Electronic Supplementary Information (ESI) available: [details of any supplementary information available should be included here]. See DOI: 10.1039/x0xx00000x

Published on 13 April 2018. Downloaded by Fudan University on 14/04/2018 14:50:12.

Journal of Materials Chemistry A Accepted Manuscript

View Article Online
DOI: 10.1039/C8TA01035J

Published on 13 April 2018. Downloaded by Fudan University on 14/04/2018 14:50:12.

properties relationship of the final catalysts. Scheme 1 illustrates the procedure for the synthesis of the bimetal/nitrogen co-doped catalysts. First, Fc-F/Co@C gel was treated by hydrothermal reaction at 150 °C for 12 h, which resulted in uniform raspberry-like nanostructures (designated as Fc-F/Co@N-C150). Subsequent pyrolysis at 800 °C generated the final bimetal and nitrogen co-doped catalysts, here denoted as Fc-F/Co@N-C800. As the precursor structure exerts great effect on the composition and activity of the final catalysts, we characterized the precursors, intermediates and final products in detail and showed as below.

Before the encapsulation of carbon, we first confirmed the formation of the Fc-F/Co bimetallogel, and further elucidated the gelation mechanism. As shown in Fig. S1, the scanning electron microscopy (SEM) reveals that both Fc-F and Fc-F/Co hydrogels are composed of nanofiber networks. However, compared with Fc-F, fibrils in the Fc-F/Co bimetallogel are much denser and thinner, suggesting that the Co^{2+} ions can further cross-link with Fc-F to form interwoven 3D networks. This is in agreement with the circular dichroism (CD) spectra, where a slight red shift can be observed as a result of coordination between Fc-F nanofibers and Co^{2+} ions (Fig. S2). In addition, fourier transform infrared spectroscopy (FT-IR) spectra were carried out to provide direct evidence for the coordination. As shown in Fig. S3, a peak at 3420 cm^{-1} (attributable to Fc-F υ_{OH} and υ_{NH} absorptions) is shifted to 3411 cm^{-1}, confirming the coordination between the Fc-F and the Co^{2+}. Furthermore, both carboxyl group at 1726 cm^{-1} and amide group at 1530 cm^{-1} undergo a red shift, indicating that both -COOH and -CO-NH- groups from Fc-F participate in the coordination with Co^{2+} ions.[28] Therefore, it can be concluded that the efficient complexation of Co^{2+} ions with -COOH and -CO-NH- groups in Fc-F promotes the gel-network formation. Surprisingly, unlike other supramolecular gel systems,[29-31] such as Fc-F, which are disassembled at high temperature, the Fc-F/Co bimetallogel could endure temperature over 100 °C, even boiling, without notable change (Fig. S4), indicative of its excellent thermostability. This is attributed to the strong coordination between metal cations and the Fc-F nanofibers, and consistent with our previous work on metal-biopolymer hydrogels, which also exhibit good thermal stability.[32]

Previous reports have shown that aromatic gelators can co-assemble with carbon materials to form hybrid gel, due to strong π-π interaction.[33-35] As the Fc-F is one of the most efficient aromatic gelators,[27, 36] we employed the Fc-F based bimetallogel as host matrix to accommodate the commercially available carbon, Ketjenblack EC 600J, which resulted in self-supporting hybrid hydrogel Fc-F/Co@C (inset of Fig. 1a). The SEM revealed that the Fc-F/Co@C bimetallogel was composed of nanofiber network, with carbon nanoparticles homogeneously attached on the nanofibers (Fig. 1a). Due to the excellent thermal stability of the Fc-F/Co@C bimetallogel, we conjectured that relatively mild thermal treatment of the gel, such as hydrothermal reaction, would allow slow decomposition of the nanofibers, leading to homogenous distribution of metal and nitrogen species within the carbon matrix. Accordingly, the Fc-F/Co@C bimetallogel was treated with hydrothermal reaction at 150 °C for 12 h. As a result, uniform raspberry-like nanospheres (denoted as Fc-F/Co@N-C150) with a diameter of about 220 nm were generated (Fig. 1b and S5). Transmission electron microscopy (TEM) reveals that these raspberry-like spheres are composed of small polycrystalline nanoparticles (inset of Fig. 1b and S6). Energy dispersive X-ray spectra (EDS) and high-angle annular dark field scanning TEM (HAADF-STEM) reveal that all the elements are homogeneously distributed over the entire architecture (Fig. S7 and S8), indicating that agglomerations of metal and nitrogen can be efficiently suppressed by the supramolecular bimetallogel templates.

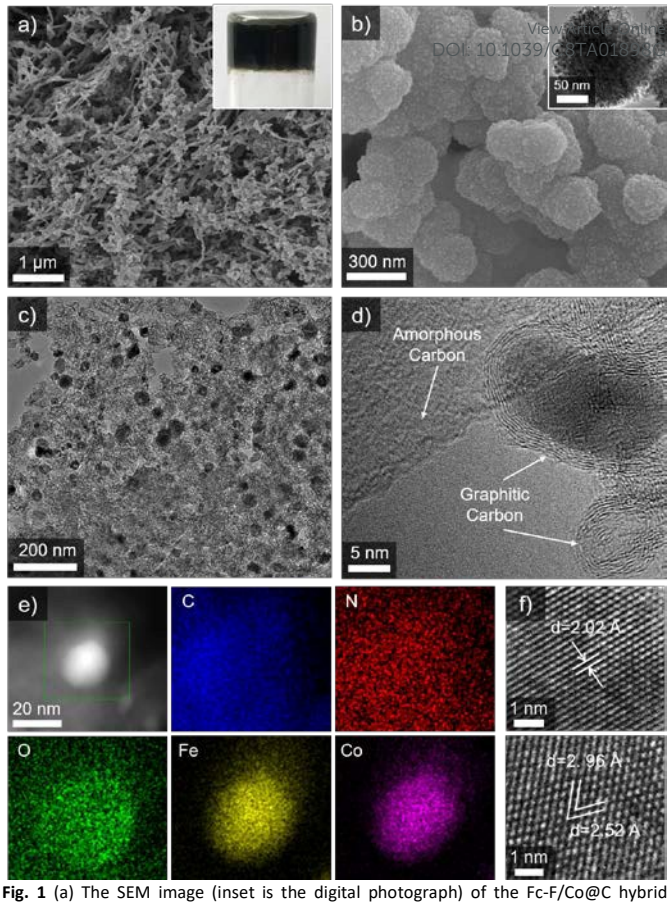

Fig. 1 (a) The SEM image (inset is the digital photograph) of the Fc-F/Co@C hybrid hydrogel; (b) SEM (inset is TEM) image of the raspberry-like Fc-F/Co@N-C150 hybrids after hydrothermal reaction at 150 °C for 12 h; (c)-(d) TEM images, (e) HAADF-STEM image and HAADF-STEM-EDS mapping of the resultant catalyst Fc-F/Co@N-C800; (f) HRTEM images of the Fc-F/Co@N-C800. The lattice distance and crystal plane angle indicate the coexistence of FeCo and $CoFe_2O_4$ nanoparticles.

To dope metals and nitrogen into carbon matrix, the Fc-F/Co@N-C150 was further pyrolyzed at 800 °C (denoted as Fc-F/Co@N-C800). As shown in Fig. 1c and 1d, nanoparticles with an average size of 28 nm were anchored homogeneously within the carbon matrix. The HAADF-STEM images in Fig. 1e shows the elemental distributions of C, N, O, Fe and Co, and a typical core-shell structure can be observed, where the elemental of Fe and Co locate in the core. This indicates the nanoparticles are encapsulated in the carbon shells, and consistent with the core-shell structures in the Fig. 1d. In addition, high-resolution TEM (HRTEM) images (Fig. 1f and S9)

Journal of Materials Chemistry A Accepted Manuscript

This journal is © The Royal Society of Chemistry 20xx

Please do not adjust margins

View Article Online
DOI: 10.1039/C8TA01889C

Published on 13 April 2018. Downloaded by Fudan University on 14/04/2018 14:50:12.

Journal of Materials Chemistry A Accepted Manuscript

of the encapsulated nanoparticles reveal that the lattice fringes of 0.296 and 0.252 nm can be assigned well to the (220) and (311) planes of cubic $CoFe_2O_4$, while 0.285 and 0.202 nm can be indexed to the (111) and (100) planes of cubic FeCo alloy. Recently, some reports have reported that the spinel-type transition metal oxides (AB_2O_4) and alloys could display high activity and good durability for electrocatalysis.[25, 26, 37-39] In contrast with the bimetallogel, samples with neither Co^{2+} nor Fc-F only resulted in serious agglomeration (Fig. S10), further signifying that the bimetallogel plays a critical role on the homogeneous doping. In addition, we also checked the temperature effect during the pyrolysis process. It was found that samples annealed at 700 °C or 900 °C produces faint or agglomerated nanoparticles in the carbon matrix (Fig. S11). Together with the electrocatalytic performances (Fig. S12), we choose 800 °C as the optimized condition hereafter.

To probe the fine structure of the Fc-F/Co@N-C800, X-ray diffraction (XRD) and X-ray photoelectron spectroscopy (XPS) were performed. As shown in the Fig. 2a and S13, XRD pattern shows that a broad diffraction peak at 26° can be observed in all samples, which attribute to the (002) planes of the graphitic carbon. We also noticed a slight shift of the peak with the addition of metal sources, possibly caused by metal doping in the carbon matrix. XPS spectra (Fig. S14 and Table S1) reveal that Fc-F can increase the contents of the metal and nitrogen residues, which may be ascribed to the effective adsorption of metal complex on the carbon surface. In the high-resolution XPS spectra (Fig. 2b), the peaks of 712.4 eV (Fe $2p_{3/2}$), 724.9 eV (Fe $2p_{1/2}$) and the shake-up satellite of 719.0 eV confirmed the presence of Fe^{3+} species. Meanwhile, the peaks around 709.5 and 722.0 eV were assigned to FeCo phase. An additional peak at 710.9 eV is ascribed to the Fe-N coordination. The existence of M-N coordination could also be seen from the Co 2p (Fig. 2c) and N 1s spectra (Fig. 2d). Thus, we can conclude that both Fe and Co are co-doped into the carbon from these measurements. Since the pyridinic N, graphitic N and M-N have been interpreted as the active sites toward ORR in considerable studies,[5, 13, 22, 40] the amount of nitrogen corresponding to active sites is calculated (Table S1). Interestingly, Fc-F/Co@N-C800 with bimetal nanoparticles and the moderate amount of active N exhibits the highest activity. This result indicates that the ORR performance cannot be simply correlated to the type of nitrogen, or the active nitrogen content, or any single factor. However, the introduction of metals into N-doped carbon system exerts an indispensable effect on the substantial improvement of the ORR activity, which could generate different intrinsic active sites, like M-N.

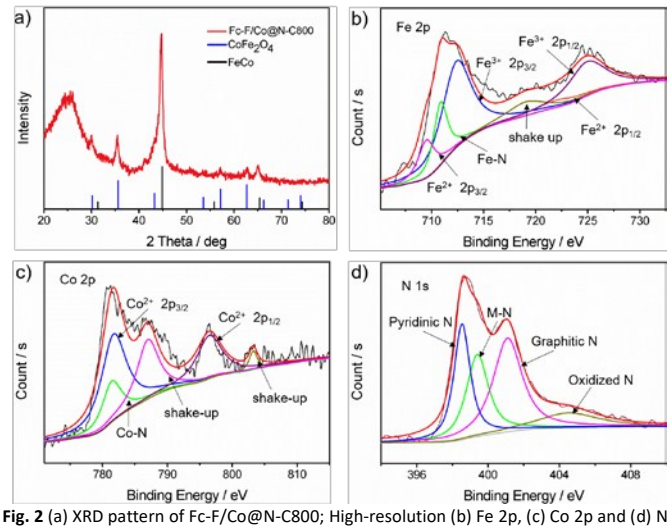

Fig. 2 (a) XRD pattern of Fc-F/Co@N-C800; High-resolution (b) Fe 2p, (c) Co 2p and (d) N 1s XPS spectra of Fc-F/Co@N-C800.

Subsequently, we evaluated the ORR performance of the resulted catalysts Fc-F/Co@N-C800. For comparison, we also prepared the Fc-F@N-C800 (without Co), Co@N-C800 (without Fc-F), Fe/Co@N-C800 (replaced Fc-F with $FeCl_3$) and C800 (simply pyrolyzed the carbon) by using the similar procedure to Fc-F/Co@N-C800 (see Experimental Section in SI). We first performed the electrical impedance spectroscopy (EIS) to measure the electrical conductivity of these materials. As shown in Fig. 3a, S15 and Table S2, the catalyst Fc-F/Co@N-C800 shows the lowest charge-transfer resistance, indicating that it exhibits the best electrical conductivity and will contribute to the fastest acceleration of electron transfer. This is possibly due to the existence of bimetal Fe and Co, which facilitates the graphitization of the carbon during the pyrolysis process. We then carried out the cyclic voltammetry (CV) to assess the ORR performance of the catalysts (Fig. 3b and S16). As expected, C800 barely exhibited obvious catalytic activity. After the introduction of bimetal Fe and Co (using metal salts instead of bimetallogel), the catalytic activity of Fe/Co@N-C800 increased to some extent, signifying the effective role of the doped bimetals. Noticeably, Fc-F/Co@N-C800 derived from the bimetallogel displays an extraordinary ORR activity with the peak potential (E_{peak}) at 0.85 V. To confirm the role of bimetal nanoparticles ($CoFe_2O_4$/FeCo) on boosting ORR catalytic activity, we examine the ORR activity of the Fc-F/Co@N-C800 after an acid leaching treatment.[40] The results of TEM and EDS (Fig. S17) confirm that metal nanoparticles are successfully removed and the nitrogen is still retained. As can be seen from Fig. S18, the acid-leached Fc-F/Co@N-C800 displays clearly inferior ORR activity with a significant peak potential shift by 51 mV. The above results reveal that the upgrade of ORR activity is attributed to the existence of the bimetal centre ($CoFe_2O_4$/FeCo). Furthermore, the Fc-F/Co@N-C800 shows better ORR property than Fc/Co@N-C800 (replac-

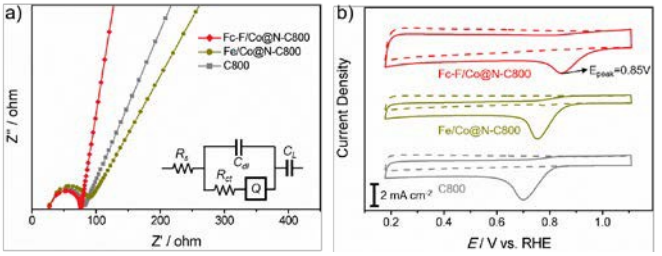

Fig. 3 (a) Nyquist plots of the as-prepared Fc-F/Co@N-C800 catalysts and the equivalent electrical circuit used for fitting impedance spectra. R_s, R_{ct} and Q are the electrolyte resistance, charge-transfer resistance and the constant phase element, respectively. C_{dl} is the double-layer capacitance, and C_L is the limit capacitance; (b) CV curves of different catalysts in O_2–saturated (solid line) and N_2–saturated (dash line) 0.1 M KOH at a scan rate of 50 mV s^{-1}.

Please do not adjust margins

View Article Online
DOI: 10.1039/C8TA01898C

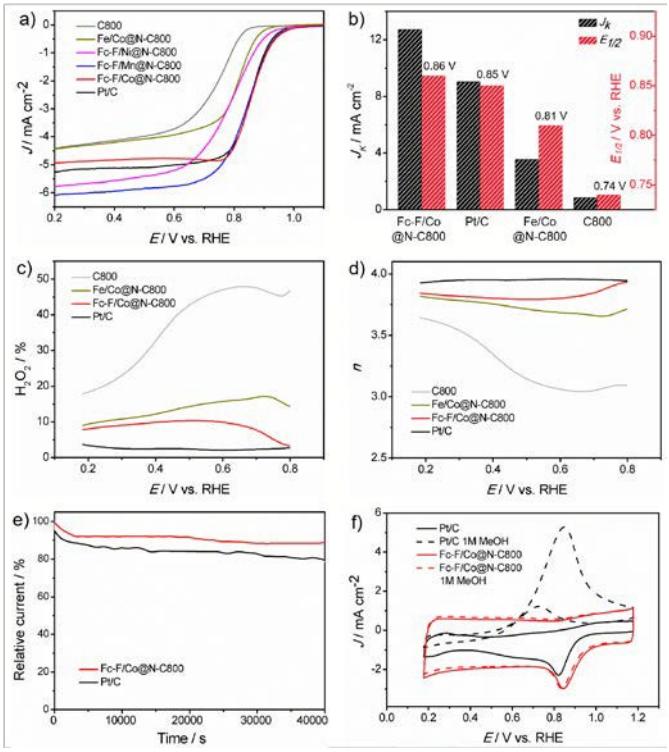

Fig. 4 (a) ORR polarization curves at 1600 rpm in O_2-sarturated 0.1 M KOH; (b) J_K at 0.80 V and $E_{1/2}$, (c) H_2O_2 yield and (d) Corresponding electron transfer number of C800, Fe/Co@N-C800, Fc-F/Co@N-C800 and 20 wt% Pt/C; (e) Chronoamperometry measurements for Fc-F/Co@N-C800 and 20 wt% Pt/C at 0.678 V, 1600 rpm; (f) CV curves of Fc-F/Co@N-C800 and 20 wt% Pt/C with or without 1 M methanol.

ed Fc-F gel with Fc powder), indicating that the supramolecular bimetallogel template is beneficial for higher electrocatalytic performance. Thus it can be concluded that the synergistic effect of the doped bimetals and nitrogen species, which they are distributed homogeneously within the carbon matrix, exerts great effect on boosting the activity of the catalysts.

A detailed study of the electrochemical activity and the mass-transfer kinetics was investigated by using rotating disk electrode (RDE) and rotating ring-disk electrode (RRDE) techniques. As shown in Fig. 4a, compared with C800 (0.86 V) and Fe/Co@N-C800 (0.92 V), the Fc-F/Co@N-C800 catalyst manifests an exceptionally high onset potential with 1.01 V, which is superior to the commercial Pt/C catalyst (0.98 V), and outperforming most of the reported MNCs catalysts (Table S3).[3, 26, 41-43] In addition, the Fc-F/Co@N-C800 catalyst also shows very larger kinetic current density (J_K) with 12.71 mA cm^{-2} at 0.80 V and high mass activity (ampere per milligram of total metal) with 0.69 A mg_{TM}^{-1} at 0.86 V (20 mV s^{-1}, Fig. 4b, S19, S20 and Table S4) , which again confirms the excellent catalytic performance of the Fc-F/Co@N-C800. RRDE tests (Fig. S21) show that the H_2O_2 yield of Fc-F/Co@N-C800 remains less than 10.39 % at all potentials (Fig. 4c), corresponding to a high average electron-transfer number (n) of 3.83 (Fig. 4d), close to that of Pt/C (3.95). The good kinetic process of Fc-F/Co@N-C800 was also confirmed by the Tafel slope in two regions (65.1 mV dec^{-1} at low overpotentials and 117.7 mV dec^{-1} at high overpotentials), closing to those of Pt/C (59.3 and 118.3 mV dec^{-1}, respectively) (Fig. S22).

Furthermore, we measure the chronoamperometry of the Fc-F/Co@N-C800 catalyst in 0.1 M KOH saturated with O_2 to check the durability. As shown in Fig. 4e, even operated at 0.678 V for 40000 s, the catalyst still retains a high relative current of 86.82%, and shows higher stability than the Pt/C. This is consistent with the CV results under continuous potentiodynamic sweeps (Fig. S23). The fuel crossover effect was also examined (Fig. 4f). In the presence of 1M methanol, the CV curves of the Fc-F/Co@N-C800 catalyst is identical to that of without methanol, showing good tolerance to methanol. However, the Pt/C presents an obvious inverse methanol oxidation peak. Because of the high activity of the as-obtained Fc-F/Co@N-C800, we further integrated the catalyst into the Al-air battery device. As shown in Fig. S24, after discharging at a constant density of 20 mA cm^{-2} for 16 h, the battery still preserves ~90 % of its activity, indicating that the Fc-F/Co@N-C800 catalyst has great potential in the Al-air batteries. Apart from the Fc-F/Co, Fc-F/Mn and Fc-F/Ni bimetallogels were also used as templates to synthesis bimetal and nitrogen co-doped carbon catalysts. Likewise, the resultant catalysts show high ORR performance in terms of E_{peak} (0.84 and 0.81 V, respectively, Fig. S25), large limited diffusion current density (6.07 and 5.77 mA cm^{-2}, respectively, Fig. 4a and S26) as well as high mass activity (0.80 and 0.72 A mg_{TM}^{-1}, respectively, Fig. S20). In addition, all the bimetal/nitrogen co-doped carbon electrocatalysts Fc-F/M@N-C800 (M=Co, Mn, Ni) show good ORR activities in 0.1 M $HClO_4$ (Fig. S27), further confirming that the 'supramolecular bimetallogel' can be an outstanding template for the in-situ synthesis of MNCs materials with excellent ORR performance.

Conclusions

In summary, we provide a rational strategy to synthesize bimetal/N co-doped carbon catalysts, using bimetallogel nanofiber network as template. Thermal treatment of the bimetallogel, hybridized with commercially available carbon, enables bimetals and nitrogen simultaneously doped into carbon matrix. Remarkably, our materials possess superior performance to commercial Pt/C benchmark for the ORR in alkaline solution, and also deliver satisfactory activity in acidic environment. Detailed electrochemical characterizations, together with XRD and XPS analysis, prove that the simultaneous doping of both bimetal and nitrogen into the carbon has a synergistic effect to boost the ORR activity. The high onset potential, large kinetic current density, high mass activity, good methanol tolerance, and long-term stability altogether make the bimetal/N-doped carbon one of the best nonprecious metal catalysts toward ORR. We believe the successful demonstration of this supramolecular bimetallogel would provide useful archetypical template for the design of other advanced electrocatalysts in energy conversion and storage systems.

Conflicts of interest

Published on 13 April 2018. Downloaded by Fudan University on 14/04/2018 14:50:12.

Journal of Materials Chemistry A Accepted Manuscript

This journal is © The Royal Society of Chemistry 20xx

There are no conflicts to declare.

Acknowledgements

This work was supported by National Nature Science Foundation of China (21473257, 21773311), the National High Technology Research and Development Program of China (2015AA020502), the Hunan Provincial Science and Technology Plan Project of China (2016TP1007), the Special Program for Applied Research on Super Computation of the NSFC-Guangdong Joint Fund (the second phase) under Grant (U1501501), the Fundamental Research Funds for the Central Universities of Central South University (2017zzts343) and Programs of Innovation and Entrepreneurship for Undergraduates (201710533507, 201710533070).

Notes and references

1. Z. W. Seh, J. Kibsgaard, C. F. Dickens, I. Chorkendorff, J. K. Norskov and T. F. Jaramillo, *Science*, 2017, **355**, 146-157.
2. D. F. Yan, Y. X. Li, J. Huo, R. Chen, L. M. Dai and S. Y. Wang, *Adv. Mater.*, 2017, **29**, 1606459-1606478.
3. A. Aijaz, J. Masa, C. Rösler, W. Xia, P. Weide, A. J. R. Botz, R. A. Fischer, W. Schuhmann and M. Muhler, *Angew. Chem. Int. Ed.*, 2016, **55**, 4087-4091.
4. Y. Jia, L. Z. Zhang, G. P. Gao, H. Chen, B. Wang, J. Z. Zhou, M. T. Soo, M. Hong, X. C. Yan, G. R. Qian, J. Zou, A. J. Du and X. D. Yao, *Adv. Mater.*, 2017, **29**, 1700017-1700024.
5. X. M. Ge, A. Sumboja, D. Wuu, T. An, B. Li, F. W. T. Goh, T. S. A. Hor, Y. Zong and Z. L. Liu, *ACS Catal.*, 2015, **5**, 4643-4667.
6. H. B. Yang, J. W. Miao, S. F. Hung, J. Z. Chen, H. B. Tao, X. Z. Wang, L. P. Zhang, R. Chen, J. J. Gao, H. M. Chen, L. M. Dai and B. Liu, *Sci. Adv.*, 2016, **2**, e1501122.
7. X. Wan, R. Wu, J. Deng, Y. Nie, S. Chen, W. Ding, X. Huang and Z. Wei, *J. Mater. Chem. A*, 2018, **6**, 3386-3390.
8. Y. Shi and G. H. Yu, *Chem. Mater.*, 2016, **28**, 2466-2477.
9. T. He, X. J. Wang, H. Q. Wu, H. Xue, P. Xue, J. Ma, M. L. Tan, S. H. He, R. J. Shen, L. Z. Yi, Y. Zhang and J. Xiang, *ACS Appl. Mater. Interfaces*, 2017, **9**, 22490-22501.
10. C. L. Zhang, B. W. Wang, X. C. Shen, J. W. Liu, X. K. Kong, S. S. C. Chuang, D. Yang, A. G. Dong and Z. M. Peng, *Nano Energy*, 2016, **30**, 503-510.
11. R. Bashyam and P. Zelenay, *Nature*, 2006, **443**, 63-66.
12. B. Cai, D. Wen, W. Liu, A. K. Herrmann, A. Benad and A. Eychmüller, *Angew. Chem. Int. Ed.*, 2015, **54**, 13101-13105.
13. Y. Y. Liu, H. L. Jiang, Y. H. Zhu, X. L. Yang and C. Z. Li, *J. Mater. Chem. A*, 2016, **4**, 1694-1701.
14. L. Z. Zhang, Y. Jia, G. P. Gao, X. C. Yan, N. Chen, J. Chen, M. T. Soo, B. Wood, D. J. Yang, A. J. Du and X. D. Yao, *Chem*, 2018, **4**, 285-297.
15. J. Wei, Y. Liang, Y. X. Hu, B. Kong, J. Zhang, Q. F. Gu, Y. P. Tong, X. B. Wang, S. P. Jiang and H. T. Wang, *Angew. Chem. Int. Ed.*, 2016, **55**, 12470-12474.
16. B. Y. Guan, L. Yu and X. W. Lou, *Adv. Sci.*, 2017, **4**, 1700247-1700252.
17. J. Ma, X. J. Wang, T. He, M. L. Tan, J. Zheng, H. Q. Wu, M. Y. Yuan, R. J. Shen, Y. Zhang and J. Xiang, *Dalton Trans.*, 2017, **46**, 6163-6167.
18. G. Wu, K. L. More, C. M. Johnston and P. Zelenay, *Science*, 2011, **332**, 443-447.
19. B. Bayatsarmadi, Y. Zheng, A. Vasileff and S. Z. Qiao, *Small*, 2017, **13**, 1700191-1700209. View Article Online DOI: 10.1039/C8TA01898G
20. T. He, H. Xue, X. J. Wang, S. H. He, Y. L. Lei, Y. Y. Zhang, R. J. Shen, Y. Zhang and J. Xiang, *Nanoscale*, 2017, **9**, 8341-8348.
21. J. Masa, W. Xia, M. Muhler and W. Schuhmann, *Angew. Chem. Int. Ed.*, 2015, **54**, 10102-10120.
22. G. Wu, A. Santandreu, W. Kellogg, S. Gupta, O. Ogoke, H. G. Zhang, H. L. Wang and L. M. Dai, *Nano Energy*, 2016, **29**, 83-110.
23. Y. Zheng, Y. Jiao, Y. Zhu, Q. Cai, A. Vasileff, L. H. Li, Y. Han, Y. Chen and S. Z. Qiao, *J. Am. Chem. Soc.*, 2017, **139**, 3336-3339.
24. S. L. Zhao, H. J. Yin, L. Du, L. C. He, K. Zhao, L. Chang, G. P. Yin, H. J. Zhao, S. Q. Liu and Z. Y. Tang, *Acs Nano*, 2014, **8**, 12660-12668.
25. W. H. He, Y. Wang, C. H. Jiang and L. H. Lu, *Chem. Soc. Rev.*, 2016, **45**, 2396-2409.
26. G. P. Wu, J. Wang, W. Ding, Y. Nie, L. Li, X. Q. Qi, S. G. Chen and Z. D. Wei, *Angew. Chem. Int. Ed.*, 2016, **55**, 1340-1344.
27. Z. F. Sun, Z. Y. Li, Y. H. He, R. J. Shen, L. Deng, M. H. Yang, Y. Z. Liang and Y. Zhang, *J. Am. Chem. Soc.*, 2013, **135**, 13379-13386.
28. S. Fleming and R. V. Ulijn, *Chem. Soc. Rev.*, 2014, **43**, 8150-8177.
29. C. H. Ren, J. W. Zhang, M. S. Chen and Z. M. Yang, *Chem. Soc. Rev.*, 2014, **43**, 7257-7266.
30. Z. A. Arnon, A. Vitalis, A. Levin, T. C. T. Michaels, A. Caflisch, T. P. J. Knowles, L. Adler-Abramovich and E. Gazit, *Nat. Commun.*, 2016, **7**, 13190-13196.
31. N. Zhou, X. Y. Cao, X. W. Du, H. M. Wang, M. Wang, S. Liu, K. Nguyen, S. Klaus, Q. B. Xu, G. L. Liang and B. Xu, *Angew. Chem. Int. Ed.*, 2017, **56**, 2623-2627.
32. Z. F. Sun, F. C. Lv, L. J. Cao, L. Liu, Y. Zhang and Z. G. Lu, *Angew. Chem. Int. Ed.*, 2015, **54**, 7944-7948.
33. B. G. Cousins, A. K. Das, R. Sharma, Y. N. Li, J. P. McNamara, I. H. Hillier, I. A. Kinloch and R. V. Ulijn, *Small*, 2009, **5**, 587-590.
34. X. W. Du, J. Zhou, J. F. Shi and B. Xu, *Chem. Rev.*, 2015, **115**, 13165-13307.
35. Y. Shi, J. Zhang, L. J. Pan, Y. Shi and G. H. Yu, *Nano Today*, 2016, **11**, 738-762.
36. K. Tao, A. Levin, L. Adler-Abramovich and E. Gazit, *Chem. Soc. Rev.*, 2016, **45**, 3935-3953.
37. G. Q. Zhang and X. W. Lou, *Adv. Mater.*, 2013, **25**, 976-979.
38. L. B. Ma, X. P. Shen, G. X. Zhu, Z. Y. Ji and H. Zhou, *Carbon*, 2014, **77**, 255-265.
39. K. W. Liu, C. L. Zhang, Y. D. Sun, G. H. Zhang, X. C. Shen, F. Zou, H. C. Zhang, Z. W. Wu, E. C. Wegener, C. J. Taubert, J. T. Miller, Z. M. Peng and Y. Zhu, *ACS Nano*, 2018, **12**, 158-167.
40. W. J. Jiang, L. Gu, L. Li, Y. Zhang, X. Zhang, L. J. Zhang, J. Q. Wang, J. S. Hu, Z. D. Wei and L. J. Wan, *J. Am. Chem. Soc.*, 2016, **138**, 3570-3578.
41. Z. H. Li, M. F. Shao, L. Zhou, R. K. Zhang, C. Zhang, M. Wei, D. G. Evans and X. Duan, *Adv. Mater.*, 2016, **28**, 2337-2344.
42. Y. Tong, P. Z. Chen, T. P. Zhou, K. Xu, W. S. Chu, C. Z. Wu and Y. Xie, *Angew. Chem. Int. Ed.*, 2017, **56**, 7121-7125.
43. P. Z. Chen, T. P. Zhou, L. L. Xing, K. Xu, Y. Tong, H. Xie, L. D. Zhang, W. S. Yan, W. S. Chu, C. Z. Wu and Y. Xie, *Angew. Chem. Int. Ed.*, 2017, **56**, 610-614.

Published on 13 April 2018. Downloaded by Fudan University on 14/04/2018 14:50:12.

Journal of Materials Chemistry A Accepted Manuscript

View Article Online
DOI: 10.1039/C8TA01898G

Published on 13 April 2018. Downloaded by Fudan University on 14/04/2018 14:50:12.

Table of Content (TOC)

Supramolecular Bimetallogels: A Nanofiber Network for Bimetal/Nitrogen Co-Doped Carbon Electrocatalysts

Minli Tan,[a] Ting He,[a] Jian Liu,[a] Huiqiong Wu,[a] Qiang Li,[a] Jun Zheng,[a] Yong Wang,[a] Zhifang Sun,*[a] Shuangyin Wang,[b] and Yi Zhang*[a]

[a.] *Hunan Provincial Key Laboratory of Efficient and Clean Untilization of Manganse Resources, College of Chemistry and Chemical Engineering, Central South University, Changsha 410083, China. E-mail: allensune@gmail.com (Z. Sun); yzhangcsu@csu.edu.cn (Y. Zhang)*

[b.] *State Key Laboratory of Chem/Bio-Sensing and Chemometrics, Hunan University, Changsha 410082, China*

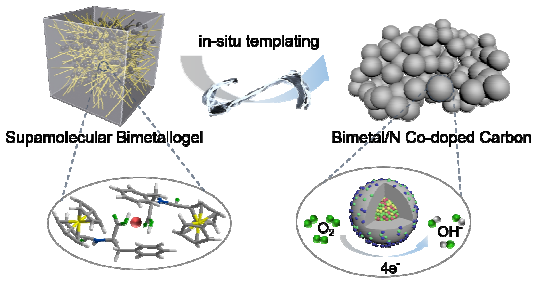

As the first example, a type of bimetal/N co-doped carbon electrocatalysts are synthesized by using 'supramolecular bimetallogel' as templates.

Journal of Materials Chemistry A Accepted Manuscript